Electronic Supplementary Information

Thermal Induced Charge Transfer in Quinoid-bridged Linear Cu_3 Compound

Xiao-Lin Liu, Xiao-Yi Zhang, Hai-Xia Zhao*, La-Sheng Long* and Lan-Sun Zheng

Collaborative Innovation Center of Chemistry for Energy Materials, State Key Laboratory of Physical Chemistry of Solid Surfaces and Department of Chemistry College of Chemistry and Chemical Engineering, Xiamen University, Xiamen 361005, P. R. China

E-mail: hxzhao@xmu.edu.cn; lslong@xmu.edu.cn

Crystal structure determination. X-ray single-crystal diffraction data were collected at different temperatures by using an Agilent Supernova CCD diffractometer in a ω-scan mode, with $\Delta\omega$ = 1.0°. The single-crystal diffraction data at 100 K and 300 K were collected by using Cu-Kα radiation (λ = 1.5418 Å). Data collection and processing were accomplished with the CrysAlis PRO program. Absorption corrections were applied by using the multi-scan program. The structures were solved and refined using full matrix least-squares based on *F2* with the SHELXS-2013/SHELXL-2013 programs within OLEX 2. The crystal data, as well as the details of data collection and refinement for the complexes, are summarized in **Table S1**. The supplementary crystallographic data for this paper are accessible at CCDC 2143793 (100 K), 2143806 (300 K). These data can be obtained free of charge from the Cambridge Crystallographic Data Centre.

Measurement of electrical properties. The temperature-dependent dielectric constants ($\varepsilon^* = \varepsilon' - i\varepsilon''$) were measured by two-probe *a.c.* impedance analysis in the frequency range of $10^{3.0}$ Hz to $10^{4.5}$ Hz (Wayne Kerr 6500B Precise Impedance Analyzer). The electric contacts were prepared by using silver paste (DAD-87) to attach 50 μm gold wires to the pressed pellets of the pure samples. The pellets were placed into a Janis cryogenic refrigeration system equipped with an American Cryomagnetics 9 T Superconducting Magnet.

Spectral acquisition. Electron paramagnetic resonance (EPR) spectra were acquired with an X-band Bruker A 300 spectrometer operating at approximately 9.4 GHz; X-ray photoelectron spectroscopy (XPS) data were acquired in an UHV

chamber equipped with an Omicron XPS (base pressure 2×10^{-10} mBar) instrument with a monochromatic aluminum anode X-ray source that supplied Kα radiation (1486.6 eV); Infrared spectra (IR) were recorded on a Nicolet AVATAR FT-IR 360 spectrophotometer with pressed KBr pellets; Ultraviolet–visible–near infrared spectroscopy measurements were performed with a UV-Vis-NIR spectrophotometer (Cary 5000) at room temperature.

Measurement of other properties. The magnetic susceptibility of the samples was measured with a Quantum Design MPMS superconducting quantum interference device (SQUID). A powder sample of **1** was analyzed under a *dc* field of 5000 Oe; Powder X-ray diffraction (PXRD) patterns were recorded on a Rigaku Ultima IV diffractiometer with Cu-*Kα* radiation (λ = 1.5418 Å) with a graphite monochromator, from 5° to 50°, at a scanning rate of 5° min^{-1}; C, H, and N microanalyses were carried out with a CE instruments EA 1110 elemental analyzer.

Computational Details:

All DFT calculations were performed in the theoretical level of UB3LYP/6-31++G(d,p)//SDD by using Gaussian 09,[1] where the initial antiferromagnetic spin population were derived from the magnetic susceptibility measurement. Concerning the effect of temperature, the initial configuration was directly obtained from X-ray single-crystal diffraction results at 300 K without further optimization.

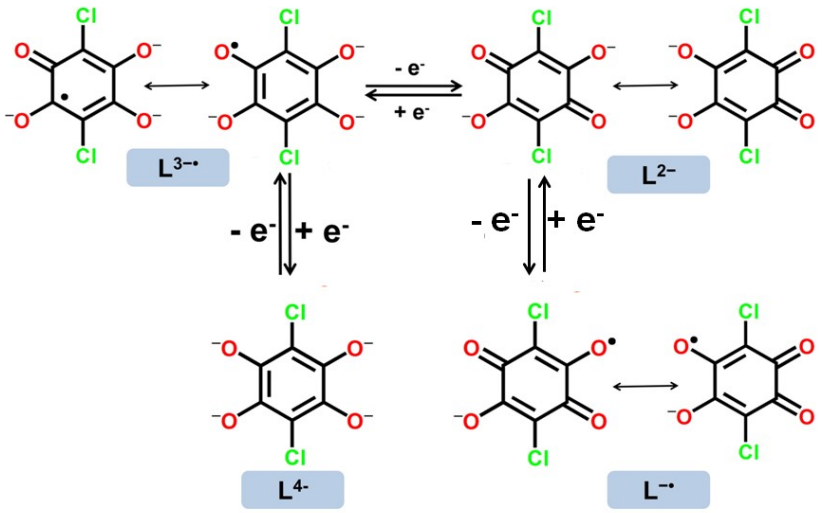

Scheme 1. Redox Series of Chloranilic Acid. $L^{3-\bullet}$ and $L^{-\bullet}$ are the paramagnetic radical bridging ligand.

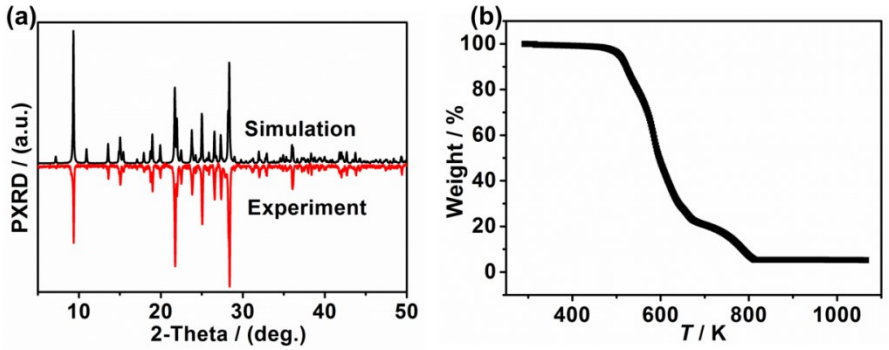

Fig. S1. (a) PXRD patterns at room temperature and (b) TG curve of **1**.

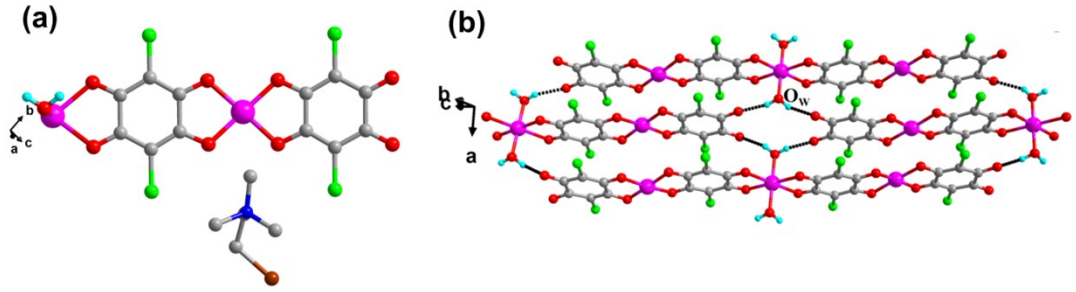

Fig. S2. The asymmetric unit of **1** at 100 K. (b) Layer structure of $[Cu_3(L)_4(H_2O)_2]^{2-}$ (dashed lines denote hydrogen bonds).

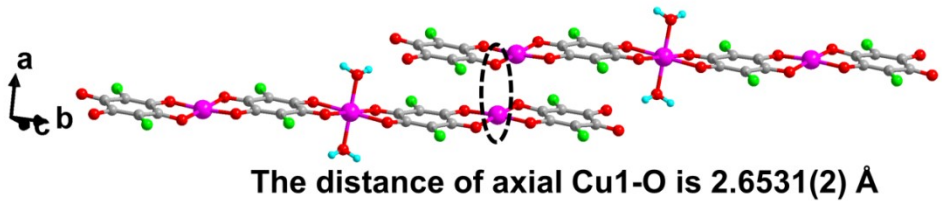

Fig. S3. The axial structure of **1**

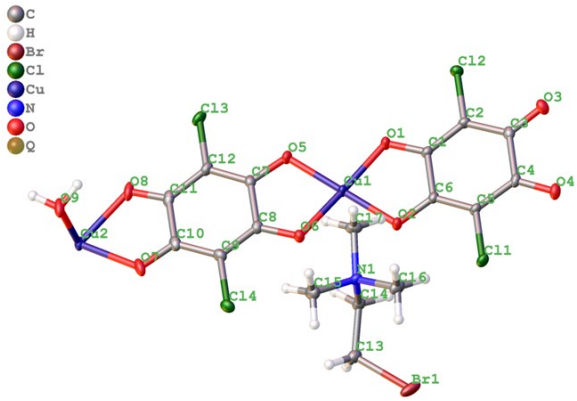

Fig. S4. The atomic label of **1**.

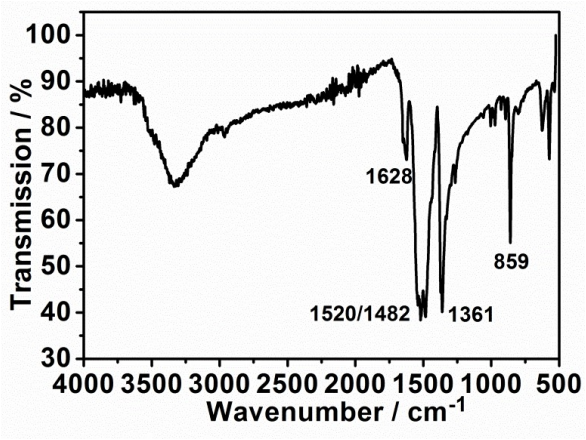

Fig. S5. Infrared spectra of **1** at room temperature.

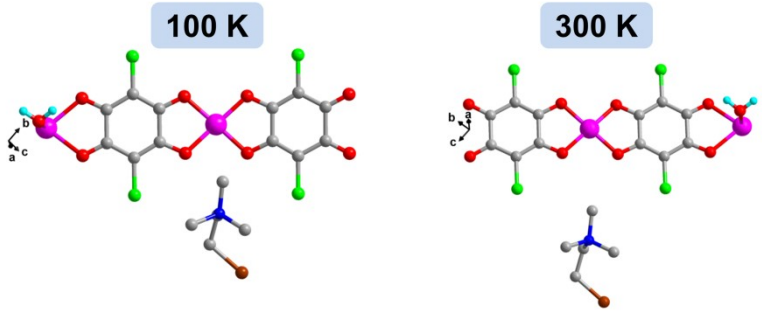

Fig. S6. The $(CH_3)_3NCH_2CH_2Br^+$ cation remained in ordered in the whole temperature range from 100 K and 300 K.

Table S1. Crystallographic data for **1** at different temperatures.

Compound	$[(CH_3)_3NCH_2CH_2Br]_2[Cu_3(Cl_2An)_4(H_2O)_2]$	
Temperature (K)	100	300
Formula weight	1388.64	1388.64
Crystal system	triclinic	triclinic
Space group	$P\bar{1}$	$P\bar{1}$
a (Å)	7.1490(2)	7.2675(2)
b (Å)	12.4532(4)	12.4908(3)
c (Å)	12.4560(4)	12.5292(3)
α (deg.)	98.008(2)	98.477(2)
β (deg.)	94.863(2)	95.120(2)
γ (deg.)	95.210(2)	95.417(2)
V (Å^3)	1088.23(6)	1113.75(5)
Z	1	1
Scan mode	ω-scan	ω-scan
ρ_{cal} (g · cm^{-3})	2.119	2.070
μ (mm^{-1})	9.081	8.873
F(000)	685.0	685.0
Crystal size (mm^3)	0.05 × 0.01 × 0.05	0.05 × 0.01 × 0.05
Radiation	Cu Kα	Cu Kα
2θ range for data collection (deg)	7.202 - 152.802	7.198 - 152.632
index ranges	$-8 \le h \le 7$ $-15 \le k \le 15$ $-15 \le l \le 15$	$-9 \le h \le 9$ $-15 \le k \le 15$ $-15 \le l \le 15$
Reflections collected	14734	10326
R_{int}	0.0367	0.0417
Refinement method	full-matrix least-squares on F^2	
Data / restraints / parameters	4506/0/308	4443 / 0 / 308
Goodness-of-fit on F^2	1.160	1.068
R_1, ωR_2 [$I > 2\sigma(I)$]	0.0413, 0.1144	0.0608, 0.1735
R_1, ωR_2 [all data]	0.0445, 0.1167	0.0644, 0.1795
Largest diff. peak/hole (e · Å^{-3})	1.25/–0.77	2.19/–1.20

$R_1 = \sum||F_o| - |F_c||/\sum|F_o|$, $\omega R_2 = \{\sum [\omega(F_o^2 - F_c^2)^2] / \sum [\omega(F_o^2)^2]\}^{1/2}$

Table S2. Selected coordination and ligand bond lengths (Å) for **1**.

Temperature	100 K	300 K
Cu1-O1	1.924(2)	1.929(3)
Cu1-O2	1.936(2)	1.921(3)
Cu1-O5	1.937(2)	1.936(2)
Cu1-O6	1.939(2)	1.931(3)
Cu2-O7	2.135(3)	2.126(3)
Cu2-O8	2.124(3)	2.127(3)
Cu2-O9	1.962(3)	1.977(7)
C1-O1	1.281(4)	1.290(4)
C6-O2	1.293(4)	1.283(4)
C4-O4	1.232(4)	1.230(5)
C3-O3	1.230(4)	1.226(5)
C8-O6	1.277(4)	1.270(5)
C7-O5	1.274(4)	1.274(4)
C10-O7	1.241(4)	1.241(5)
C11-O8	1.245(4)	1.234(5)

Table S3. Equivalent isotropic displacement parameters ($Å^2$) of coordinated water for **1**.

Temperature	100 K	300 K
O(H_2O)	0.0228(5)	0.0493(8)

Table S4. Equivalent isotropic displacement parameters ($Å^2$) of $(CH_3)_3NCH_2CH_2Br^+$ cation for **1**.

Temperature	100 K	300 K
Br1	0.0278(13)	0.0815(3)
N1	0.0146(5)	0.0339(7)
C13	0.0195(7)	0.0528(11)
C14	0.0159(6)	0.0380(8)
C15	0.0204(7)	0.0558(12)
C16	0.0166(7)	0.0535(11)
C17	0.0136(6)	0.0522(11)

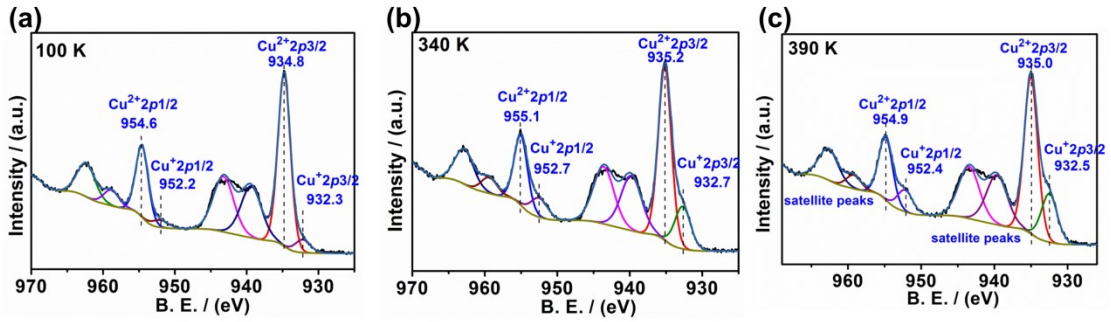

Fig. S7. Temperature-dependent XPS survey spectrum of **1** from 100 to 390 K.

Table S5. The percentage content of Cu^{II} and Cu^{I} was obtained by XPS peak area fitting.

	Cu^{II} (%)	Cu^{I} (%)
100 K	95.6	4.4
300 K	88.3	11.7
340 K	85.9	14.1
390 K	73.3	26.7

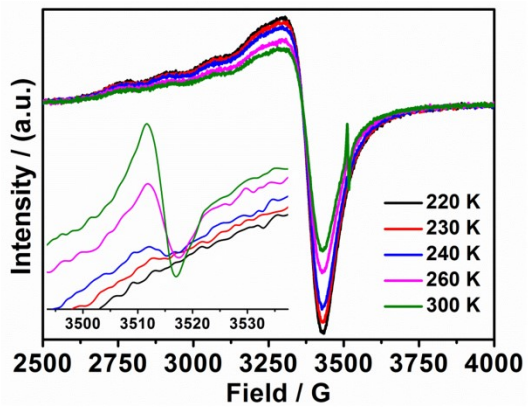

Fig. S8. EPR spectra of **1** in the temperature range of 220–300 K.

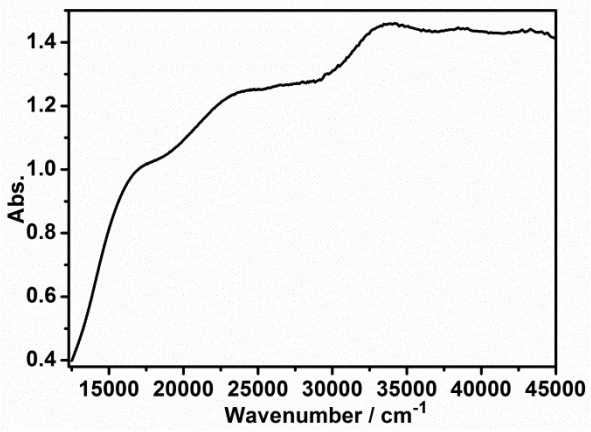

Fig. S9. UV-Vis-NIR spectra of **1** at room temperature.

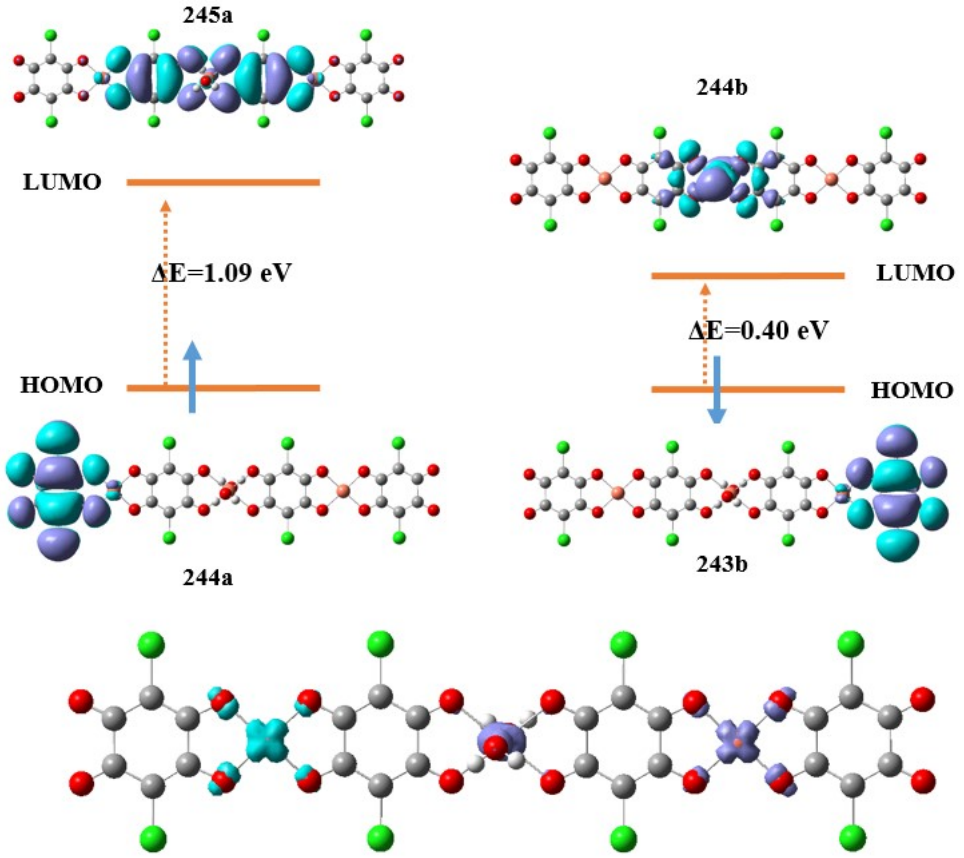

Fig. 10. (a) Two possible transitions for thermal charge transfer; (b) spin density of **1** with the 0.01 au isovalue.

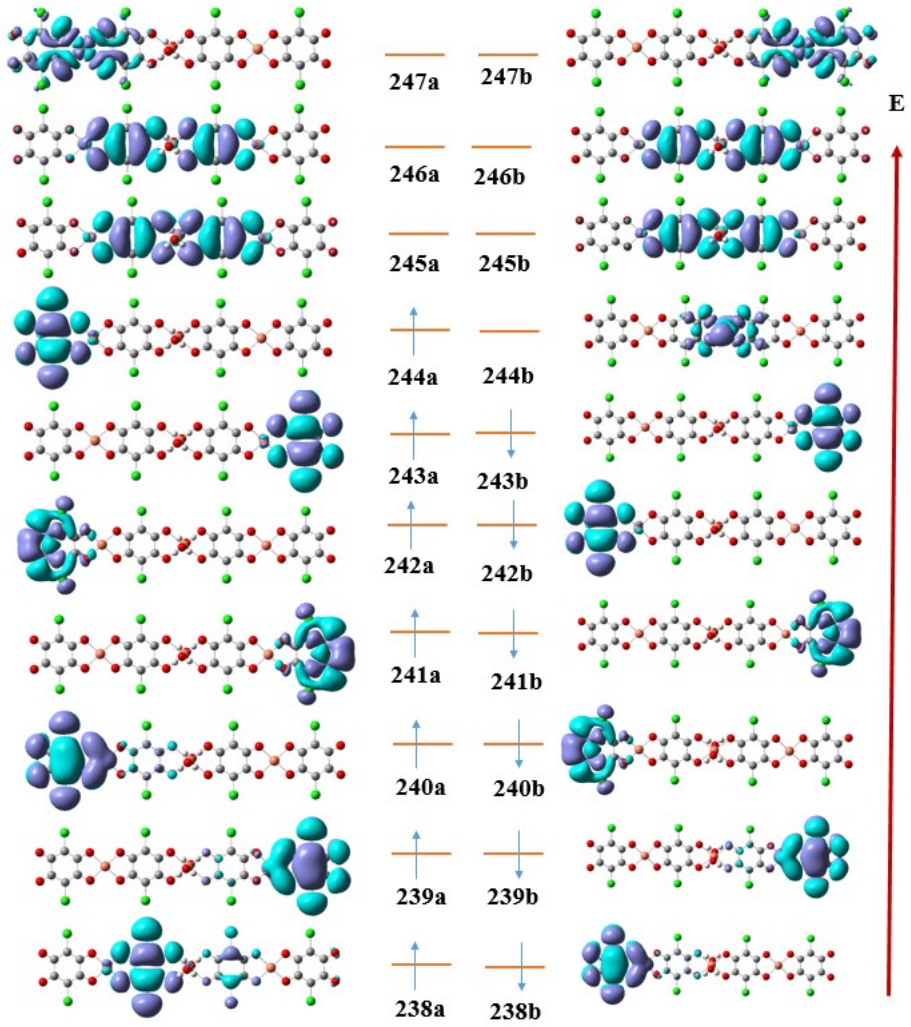

Fig. S11. Frontier molecular orbitals of **1** with spin up (labelled as a) and spin down (labelled as b) with the 0.01 au isovalue.

References:

1. Gaussian 09, Revision A.1, M. J. Frisch,et.al Gaussian, Inc., Wallingford CT, 2009.